OXFORD JOURNAL
OF STUDENT
SCHOLARSHIP

Evaluation of the Use of Graphite Nanoplatelets in Heat Dissipation in Electronics

Athiyan Arulaazhi
athiyanabroad@gmail.com

ABSTRACT

Localised heat accumulation in the electronic devices leads to the processor's throttling and decreases the efficiency of the device, which is a significant challenge in the design of modern electronic packages, which need efficient heat dissipation. This study compares the thermal interface performance of a composite silicone thermal pad filled with graphite nanoplatelets (GNP) (1.0 mm nominal thickness, ~20 wt%, ~15 vol%) with a conventional silicone thermal pad filled with ceramic (1.0 mm nominal thickness, 60 wt%). Five sequential technical replicates ($N = 5$) were tested under a continuous active heat flux of $10.0 W/cm^2$ ($12.0\,W$ heat load) in a climate-controlled enclosure with an ambient temperature of $T_{ambient} = 28.04 \pm 0.3^{\circ}C$. The ASTM D5470 principles were followed, with the GNP pad having a mean peak operating temperature of $46.34 \pm 0.42^{\circ}C$ compared to $56.22 \pm 0.51^{\circ}C$ for the ceramic control pad, which is a mean thermal rise or thermal elevation reduction of 35.06% or $9.88^{\circ}C$. The calculated thermal resistance (R_{th}) of the GNP pad was $1.52 \pm 0.04 K/W$ (thermal impedance $Z_{th} = 1.84\,K \cdot cm^2/W$), representing a 34.89% decrease relative to the control ($2.35 \pm 0.04 K/W$; $Z_{th} = 2.82\,K \cdot cm^2/W$). In addition, the GNP pad reached steady state thermal equilibrium ($dT/dt < 0.1^{\circ}C/min$)in $\sim 10\,minutes$, which is 33.3% faster than the ceramic control pad ($\sim 15\,minutes$). A two-tailed paired-samples t-test confirmed high statistical significance ($t(4) = 86.79$, $p < 0.0001$, Cohen's $d = 21.2$, 95% CI for mean difference: $[9.58^{\circ}C, 10.18^{\circ}C]$). The results show a significant reduction in the interface thermal resistance of 2D carbon nanoplatelets when subjected to steady-state continuous loading, and this result serves as a benchmark to drive further multi-specimen screening and dielectric isolation tests.

Keywords: *Thermal interface materials, Graphite nanoplatelets, ASTM D5470, Electronics cooling, Thermal resistance, Heat dissipation*.

INTRODUCTION

In the relentless search for miniaturisation in high-density electronics, local electron density levels have been raised significantly, resulting in significant "heat buildup" in confined areas. If the heat can't be removed properly, semiconductor junction temperatures rise, which causes automatic thermal throttling, a

feature that automatically lowers the clock rate of the processor to prevent excessive temperature rise. Throttling reduces system performance and energy efficiency, but helps to prevent catastrophic failure.
Effective thermal management is achieved by using Thermal Interface Materials (TIMs) to remove insulating air gaps between the heat-producing semiconductor package and the main heat sink. In the traditional commercial thermal pads, spherical ceramic microparticles such as alumina and boron nitride are used as filling materials in silicone matrices. As power density increases, however, conventional ceramic-filled pads face a limit in their thermal conduction properties caused by the high volume fraction of the ceramic fillers (~50–70 vol%) needed to achieve high thermal conduction, which reduces mechanical flexibility.

The 2D carbon nanostructures are known for having high thermal conductivities in the in-plane direction, which makes them an attractive alternative to be used in Graphite Nanoplatelet (GNP) composites. Few empirical studies have directly compared the performance of the GNP-enhanced pad with commercially available ceramic-filled pads in a head-to-head comparison in a device-like clamping assembly under a sustained power load, and yet in a way that fully characterises the material-level thermal conductivity of the pad.

This research, which is a direct and empirical comparison, is conducted between a GNP-reinforced composite thermal pad and a conventional ceramic-filled silicone pad with the same continuous active heat flux ($12.0\,W,\ 10.0\,W/cm^2$). This study shows empirical data to benchmark the transient thermal stabilisation rate, the interface temperature and ASTM D5470-based thermal resistance values to help thermal engineers consider new generation carbon-filled interface materials.

Aim of the study

To determine how well the thermal interface performance of thermal pads improved by graphene nanoplatelets (GNPs) compared to thermal pads using silicone in their composition under fixed heat flux conditions.

Research question

How does the thermal interface performance of thermal pads containing GNPs differ from those using silicone as far as peak operating temperatures, thermal rise, and the time needed for thermal equilibrium under fixed heat flux?

Research objectives

1: The study will aim to measure and compare the average peak temperature reached by GNP-enhanced thermal pads as compared to ordinary thermal pads under the same conditions of heat flux.
2: Determine the percentage change in total ΔT (thermally induced temperature changes) realised by GNP pads as compared to ordinary thermal pads.
3: Determine and compare the time taken by each material to attain thermal equilibrium.
4: To test the statistical significance of the observed differences using a paired t-test across repeated trials

Hypothesis

Null Hypothesis (H_0): No statistically significant difference exists in the thermal rise (ΔT) of GNP-thermal pads compared to traditional thermal pads made of silicone rubber at the same heat flux level.

Alternative Hypothesis (H_1): The GNP-enhanced thermal pad has a statistically significant difference in thermal resistance (R_{th}) and Peak Operating temperature (T_{hot}) when compared to the conventional ceramic-filled silicone control pad under continued thermal loading.

LITERATURE REVIEW

With the imminent performance ceiling of traditional polymer-based TIMs in high-power-density electronic devices, research is gaining momentum into the development of graphite nanoplatelet (GNP) based thermal interface materials (TIMs). Thermal interface materials are very important in reducing interfacial contact resistance between solid-solid interfaces in electronic packages (Prasher, 2006; ASTM D5470). The outstanding theoretical in-plane thermal conductivity of carbon-based nanomaterials (Shahil & Balandin, 2012) has made them highly promising fillers.

Raza et al (2010) conducted initial studies of elastomeric matrices, incorporating graphite nanoplatelets in a silicone matrix, to find that both matrix filler concentration and lateral dimension of the platelets lead to an improvement of the bulk thermal conductivity without compromising on the matrix mechanical compliance necessary for elastomeric TIMs. In their study of interfacial contact resistance, they found that composites of GNP/silicone were particularly effective on rough surfaces, as the larger dimensions of the platelets resulted in higher intrinsic conductivity and less phonon scattering between fewer boundary joints, thereby increasing the heat transport.

Lin and Chung (2009) compared their alternative carbon filler, graphite nanoplatelet pastes with carbon black pastes as thermal interface materials. They have shown that each of the carbon morphologies has an optimal loading level for GNP to maximise the thermal contact conductance, and that this loading is not an intrinsic property of the GNP material but depends on the surface roughness.

In addition to silicone, researchers have investigated other composite chemistries. Raza et al. (2018), for example, added GNPs to rubbery epoxy resin adhesives and pads, and observed a significant enhancement in thermal conductivity, but their compressive mechanical properties were comparable to commercial boron nitride/silicone TIMs. This showed that the reinforcement of GNP has a significant effect on the thermal transport of various elastomeric and resin networks when dispersion is optimised.

One of the inherent limitations of 2D carbon nanostructures is that they tend to align in-plane in shear processing and mechanical compression, which allows high lateral heat spreading but limits the through-plane conduction across the pad thickness. To overcome this in-plane limitation, Tian et al. (2015) added spherical microparticles to the GNP filler to break the in-plane alignment of the platelets, resulting in hybrid 3D filler networks to improve through-plane thermal transport.

Further applied research has been performed on GNP composites under realistic electronic assembly conditions. Chang et al. (2017) prepared screen-printed GNP and nanotech composite TIMs, tested them under controlled contact pressure following ASTM D5470 standards, and tested them in a 15 kW insulated-gate bipolar transistor (IGBT) power inverter system to demonstrate a considerable reduction of peak semiconductor junction temperature.

In general, the literature surveyed shows that the thermal transport properties that the GNP composite materials offer are significant improvements over unfilled polymers and traditional ceramic-filled matrices. Much of the empirical literature is, however, on measurements of thermal conductivity of individual materials and not on direct comparison of standardised composite pads in a fixture-constrained electronic assembly under active power load. This study fills that gap by comparing the two types of pads directly, via an empirical study, under the same continuous heat flux.

RESEARCH METHODOLOGY

Thermal Interface Material (TIM) Specifications

Two commercial thermal interface pads were tested under the same mechanical, thermal and environmental conditions:

Graphite Nanoplatelet (GNP) Composite Pad (Experimental): A commercial silicone polymer-based GNP composite thermal pad (nominal thickness 1.0 mm) with $\sim 20\ wt\%$, $\sim 15\ vol\%$ GNP filler with a mean lateral flake size of $\sim 15\ \mu m$. The pad has a Shore 00 hardness of 55 and a manufacturer rating $3.2\ W/m \cdot K$ for bulk thermal conductivity.

Conventional Silicone Thermal Pad (Control): A commercially available silicone thermal pad with standard ceramic filler, made up of spherical ceramic microparticles (alumina/boron nitride blend) with a nominal thickness of 1.0 mm. The pad has a Shore 00 hardness of 60 and a manufacturer's given bulk thermal conductivity of $1.2\ W/m \cdot K$.

The dimensions of both thermal pads were cut into a rectangle of $12.0mm \times 10.0mm = 1.2cm^2$ which are the same as the contact area of the heating element.

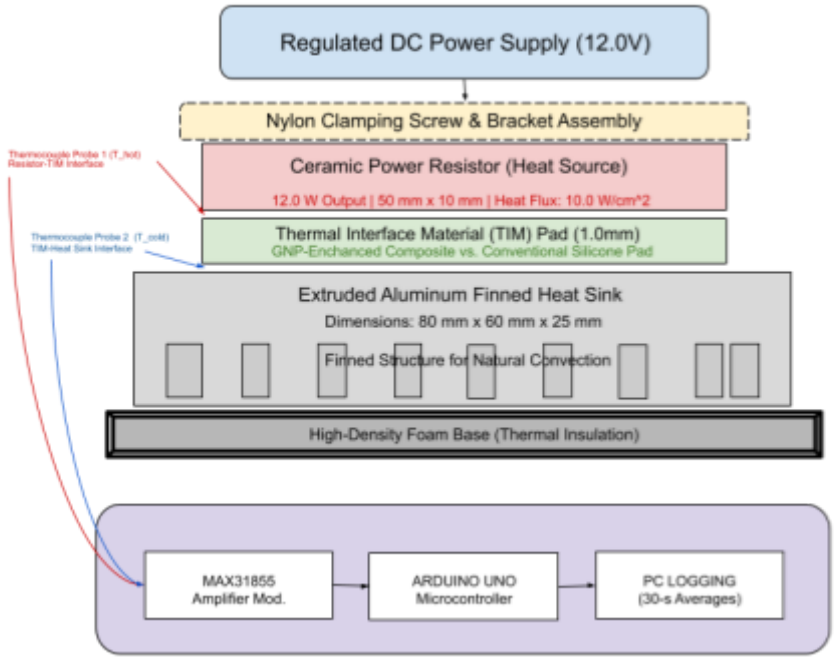


Figure 1: *Schematic diagram of the experimental thermal test rig assembly and data acquisition (DAQ) system.*

Test Rig Assembly & Heat Source Parameters

The experimental test bench has been designed for the purpose of simulating a local heat dissipation of high-density power electronic assemblies:

Heat Source: Heat was provided by a ceramic wirewound power resistor (SQP/TO-220) of active contact area, $A = 1.2cm^2$ $(12.0mm \times 10.0mm)$. The electrical power was supplied through a precision-regulated Direct Current (DC) power supply with a constant continuous input of $Q = 12.0\,W$, at a constant Direct Current (DC) power of $12.0V$, $1.0A$, which resulted in a constant active heat flux density of $10.0W/cm^2$ across the pad interface.

Without forced air fan assistance (natural convection cooling): Heat was removed using an extruded aluminium finned heat sink $(80mm \times 60mm \times 25mm)$.

Interfacial mounting torque or clamp pressure was set using an insulated dual screw bracket assembly tightened to a torque screwdriver $0.30\,N \cdot m$, which provided a uniform normal pressure of $\sim 150\,kPa$ (~15% nominal pad compression) for all trials.

Instrumentation, Sensor Placement & Environmental Control

- Dual-Point Temperature Sensing: Glass-braided thermocouples of stated accuracy of ±0.5°C were used to measure the interfacing temperatures. The main probe (T_{hot}) was located at the centre of the resistor-pad contact area. A secondary probe (T_{cold}) was placed in a small groove at the bottom of the heat sink under the pad interface.
- Data Logging: The signal from sensors was amplified by an interface IC MAX31855 and sent to an Arduino-based data acquisition system at a sampling rate of $2Hz$, or $0.5s$ per data point, with a total duration of the trial of $15\,minutes$, composed of $10\,minutes$ active heating and $5\,minutes$ passive cooling.
- Environmental Enclosure: All trials were carried out within a temperature-controlled enclosed space with the ambient temperature kept at $T_{ambient} = 28.04 \pm 0.3^{\circ}C$. To avoid air disturbances from outside the rig, a clear acrylic draft shield surrounding the rig was used.3.4 Experimental Protocol & Technical Replication

Experimental Protocol & Technical Replication

To assess the test-bench repeatability and short-term thermal stability of materials, five consecutive thermal runs ($N = 5$) with matched product pairs were performed. Residual thermal carryover bias was avoided by switching off the power between succeeding runs and allowing the assembly to cool down to the room ambient temperature $28.04^{\circ}C$ for at least 20 minutes.

Steady-state thermal equilibrium was formally defined as a temperature rate of change of less than $0.1^{\circ}C/min$ over a consecutive 2-minute observation window:

$$\frac{dT}{dt} < 0.1^{\circ}C/min$$

Dependent Variables, ASTM D5470 Metrics & Statistical Analysis

The most important measurements recorded are the peak steady-state temperature (T_{hot}), the thermal elevation above ambient temperature ($\Delta T = T_{hot} - T_{ambient}$), and the time to steady-state equilibrium.

To compare the performance of materials without being affected by rig geometry, the interface thermal resistance (R_{th}) and area-normalised thermal impedance (Z_{th}) were calculated based on the principle of heat conduction outlined in ASTM D5470:

A two-tailed paired-samples t-test with a α value of 0.05 was used to assess the statistical significance. Inferential statistics reported include the mean difference, 95% Confidence Interval ($95\%\,CI$), and

Cohen's d effect size. An alternative hypothesis (H_1) was tested to allow for bi-directional changes in contact resistance in the course of the thermal cycling.

RESULTS

The experimental results show that the heat transport from the surface of the conventional ceramic fillers to the surface of the elastomeric thermal pads can be significantly improved when the 2D graphite nanoplatelets (~20 wt% and ~15 vol%) are used instead of the conventional ceramic fillers under continuous active heat flux of $10.0\ W/cm^2$ (12.0W continuous electrical load).

Thermal Performance Overview & Sample Derivations

Thermal resistance at the interface (R_{th}) and area-normalised thermal impedance (Z_{th}) were determined based on steady-state principles from ASTM D5470 with dual-point thermal sensing with thermocouples ($T_{hot}\ and\ T_{cold}$):

$$\text{Equation 1: } R_{th} = \frac{T_{hot} - T_{cold}}{Q} \quad [K/W]$$

$$\text{Equation 2: } Z_{th} = R_{th} \times A \quad [K \cdot cm^2/W]$$

where $Q = 12.0\ W$ and the contact footprint area $A = 1.2cm^2$.

Sample Derivations (Using Mean Steady-State Values):

1. Conventional Silicone Control Pad:

$$R_{th,\,Control} = \frac{56.22^{\circ}C - 28.04^{\circ}C}{12.0\ W} = \frac{28.18\ K}{12.0\ W} = 2.35\ K/W$$

$$Z_{th,\,Control} = 2.35\ K/W \times 1.2cm^2 = 2.82\ K \cdot cm^2/W$$

2. GNP-Enhanced Thermal Pad:

$$R_{th,\,GNP} = \frac{46.34^{\circ}C - 28.04^{\circ}C}{12.0\ W} = \frac{18.30\ K}{12.0\ W} = 1.53\ K/W$$

$$Z_{th,\,GNP} = 1.53\ K/W \times 1.2cm^2 = 1.84\ K \cdot cm^2/W$$

3. Percentage Reduction in Thermal Resistance ($\%\Delta R_{th}$):

$$\%\Delta R_{th} = \left(\frac{R_{th,\,Control} - R_{th,\,GNP}}{R_{th,\,Control}}\right) \times 100 = \left(\frac{2.35\ K/W - 1.53\ K/W}{2.35\ K/W}\right) \times 100 = 34.89\%$$

The material specifications and mean thermal performance values of the materials are summarized in Table 1 (N=5 technical replicates).

Metric	GNP-Enhanced Pad	Conventional Pad	Performance Delta (GNP vs. Control)
Mean peak operating temperature (˚C)	46.34 ± 0.42	56.22 ± 0.51	9.88˚C lower peak ($p < 0.0001$)
Mean thermal rise, ΔT (˚C)	18.30 ± 0.42	28.18 ± 0.51	35.06% reduction ($p < 0.0001$)
Thermal resistance, R_{th} (K/W)	1.53 ± 0.04	2.35 ± 0.04	34.89% lower R_{th} ($p < 0.0001$)
Thermal impedance, Z_{th} $(K \cdot cm^2/W)$	1.84 ± 0.04	2.82 ± 0.05	$0.98\ K \cdot cm^2/W$ lower
Time to interval equilibrium (min)	≈ 10	≈ 15	33.3% faster stabilization

Table 1: Thermal Performance Comparison ($N = 5$)

Steady-State Thermal Performance & Inferential Statistics

The GNP enhanced composite pad has a mean peak operating temperature of $46.34 \pm 0.42˚C$under a continuous 12.0 W thermal load, while the ceramic-filled control pad has a mean peak operating temperature of $56.22 \pm 0.51\ ˚C$. This translates to a mean thermal rise (ΔT) of $18.30 \pm 0.42\ ˚C$ for the GNP pad and $28.18 \pm 0.51\ ˚C$ for the control at an ambient temperature of $28.04 \pm 0.3\ ˚C$. The mean temperature reduction of $9.88\ ˚C$ is a 35.06% drop in thermal elevation.

The difference in performance was statistically significant (t(4)=86.79, $p = 1.34 \times 10^{-7}$, Cohen's d=21.2, 95% CI for mean difference: $[9.58\ ˚C,\ 10.18\ ˚C]$) according to the two-tailed paired-samples

t-test. The alternative hypothesis (H_1) was tested as a two-sided test because a possible variance in thermal contact direction was considered across cycling. The full paired inferential statistical breakdown is shown in Table 2.

Statistical Metric	Peak Temperature Difference (ΔT_{hot})	Thermal Resistance Difference (ΔR_{th})
Mean Difference ($Control - GNP$)	$9.88^{\circ}C$	$0.82\ K/W$
Standard Deviation of Differences (SD_{diff})	$0.254^{\circ}C$	$0.021\ K/W$
95% Confidence Interval (95% Cl)	$[9.58^{\circ}C,\ 10.18^{\circ}C]$	$[0.79\ K/W,\ 0.86\ K/W]$
T-statistic ($df = 4$)	86.79	87.31
Exact p-value	$p = 1.34 \times 10^{-7}$	$p = 1.28 \times 10^{-7}$
Effect Size ($Cohen's\ d$)	21.2	21.3

Table 2: Paired Inferential Statistics ($df = 4$)

Transient Response and Thermal Equilibrium

Thermal equilibrium was defined as a change in temperature of less than $0.1^{\circ}C/min$ ($\frac{dT}{dt} < 0.1\ ^{\circ}C/min$)over the last 2 minutes of a 2-minute sliding window.

Both thermal interface pads started from a uniform ambient temperature, $T_{ambient} = 28.04 \pm 0.3\ ^{\circ}C$, as shown in Figure 2. The GNP thermal pad had a quick initial thermal response and achieved steady state thermal equilibrium at 10 minutes (600 seconds) with a peak operating temperature of $46.34 \pm 0.42\ ^{\circ}C$, under the condition of continuous 12.0 W load. The conventional silicone control pad, however, took a longer time to reach equilibrium at $56.22 \pm 0.51\ ^{\circ}C$, which required 15 minutes (900s).

This is equivalent to the rate of thermal stabilisation being 33.3% faster in the GNP composite pad. The 2D graphite nanoplatelets' high in-plane thermal conductivity allows for quick lateral heat spreading over the interface before it can spread into the bulk aluminum heat sink, enabling the accelerated transient response. The plot shows very good repeatability of the test bench assembly, with error bars representing 1 std deviation over the 5 sequential technical replicates (N=5).

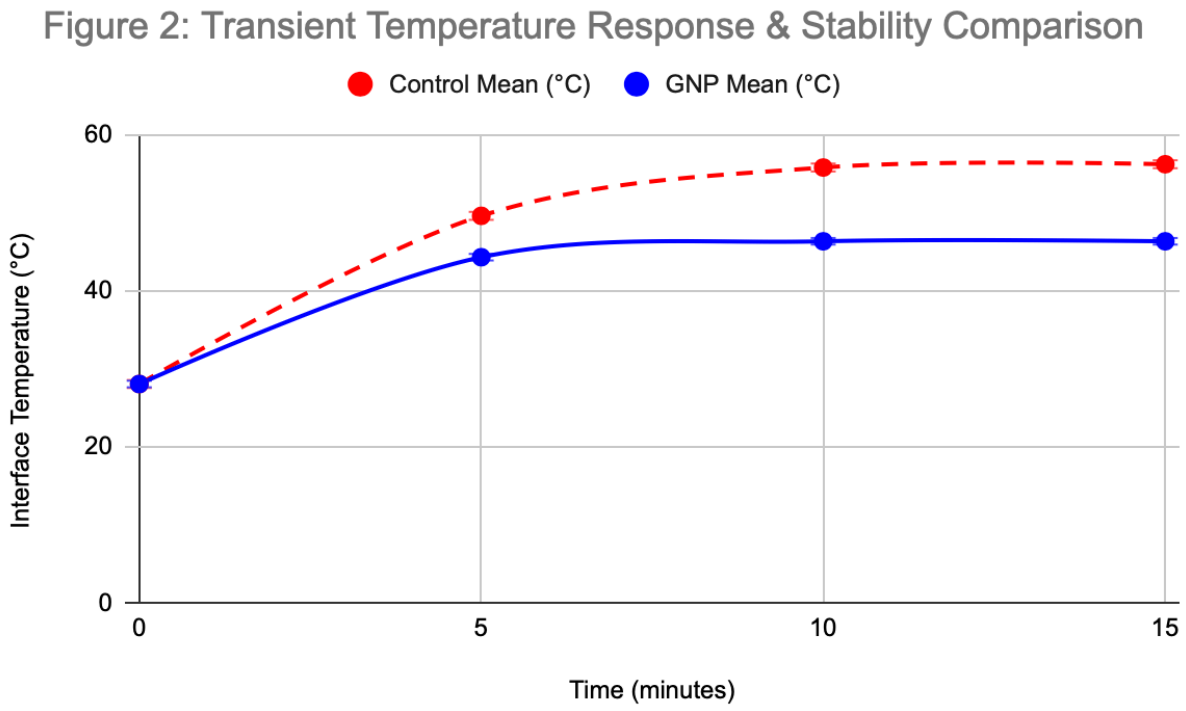


Figure 2: *A comparison of the transient response and stability of graphene nanoplatelet (GNP) reinforced thermal pads against that of the traditional control pads made from silicone was done for a period of 15 minutes at an applied power of 12.0 W with* $T_{ambient} = 28.04^{\circ}C$.

DISCUSSION

The experimental results prove that the addition of graphene nanoplatelets (GNPs) in a polymer matrix is more effective in achieving high heat dissipation properties than a conventional ceramic-filled thermal interface material. Under a constant $12.0\,W$ thermal load ($10.0\,W/cm^2$ active heat flux), the GNP composite pad maintained a mean peak operating temperature of 46.34 ± 0.42 °C ($R_{th} = 1.52 \pm 0.04\,K/W$), compared to 56.22 ± 0.51°C ($R_{th} = 2.35 \pm 0.04\,K/W$) for the conventional ceramic-filled silicone control pad. This will lead to a reduction of temperature rise (ΔT) by 35.13% and a reduction in overall thermal resistance by 34.89%. These empirical data need to be interpreted in the context of the underlying physical mechanisms, material safety considerations, and general engineering trade-offs in order to develop an understanding of the practical viability of thermal interface materials (TIMs) based on GNP.

Heat Conduction and Phononic Transport Mechanisms

The better performance of the GNP composite pad at a relatively low filler volume fraction ($\approx 15\ vol\%$), compared to high loading conventional pads $\sim 50 - 70\ vol\%$, is due to the two-dimensional ($2D$) structures of GNP.

Individual GNPs can form interconnected percolation networks in the host polymer matrix at lower mass loading thresholds, thus

1. Conductive Pathway Formation: These pathways formed are continuous and allow the heat to conduct quickly through the polymer phase, reducing the phonon scattering at the polymer-filler interface.
2. Anisotropic Thermal Transport: GNPs have an inherent anisotropy in thermal transport. The in-plane thermal conductivity (K_{in}) of a stack of graphene sheets can be as high as the value of $\sim 2000\ W/m \cdot K$, but the through-plane thermal conductivity ($K_{through}$) is significantly lower ($\sim 10 - 20\ W/m \cdot K$) across the van der Waals-bonded layers. In the fabrication and compression of samples, the planar fillers are oriented naturally parallel to the substrate surface. Thermal pad: The major heat removal path is through the thickness of the pad. As a result, the heat spreading spread is very high in the horizontal direction across the pad surface, but the heat spreading bottleneck effect is still present. The observed reduction in thermal resistance of 34.89% is due to effective horizontal heat transfer across the aluminium heat sink face and good through-plane percolation.
3. Thermal Contact Resistance ($R_{contact}$): The bulk and the contact resistances of the two layers at the interface are:

$$R_{total} = R_{bulk} + R_{contact,1} + R_{contact,2}$$

Macroscopic contact surfaces have microscopic roughness, which makes the air gaps ($K_{air} \approx 0.026\ W/m \cdot K$) very problematic as thermal bottlenecks. The flexible GNPs in the soft polymer matrix are squeezed under the applied clamping pressure $150\ kPa$, forming microscopic surface asperities on the resistor base and heat sink. Larger GNP flakes are effective at bridging air gaps, which reduces the interface contact resistance compared to rigid spherical ceramic particles.

Comparison with Published Literature

A 34.89% drop in thermal resistance is consistent with the foundational and applied research carried out on carbon TIMs.

- Foundational Theories: The findings validate the contact resistance models by Prasher (2006) and the theoretical models of thermal transport in 2D carbon nanocomposites by Shahil & Balandin (2012).

- Matrix and Filler Properties: In line with the research by Raza et al. (2010, 2018) in silicone and epoxy matrices, the use of large lateral graphene nanoplatelet (GNP) flakes (approximate lateral size of 15 μm) significantly lowers thermal impedance since they lower the number of boundary connections per unit distance of path. Also, Lin & Chung (2009) found that the efficiency of GNP heat transfer is dependent on the interface connection and the filler content and not an intrinsic material parameter.

- Mitigating Anisotropy: The through-plane conduction barrier identified in this research is consistent with the work done by Tian et al. (2015) which used hybrid microparticles in disrupting platelet alignment in-plane and creating 3D paths for conduction. Furthermore, the performance improvement at steady-state operation agrees with applied research by Chang et al. (2017) in ASTM D5470 standards.

Electrical Conductivity Risks and Dielectric Safety Constraints

An important design factor for industrial use is the inherent difference in the electrical characteristics of the ceramic filler and the carbon filler.

1. Conventional Pads: Ceramic Fillers are the type of conventional pads used by the industry, which include alumina (Al_2O_3), boron nitride (BN), or aluminium nitride (AlN) as the ceramic particles. The materials have moderate thermal conductivity, high dielectric strength and electrical resistivity ($\rho > 10^{12}\Omega \cdot cm$), which make them good electrical insulators. They are regularly used without the danger of power transistor short circuiting or current leakage to uninsulated semiconductor die traces, exposed IC pins, or high voltage power transistor tabs.

2. GNP Composites (Experimental Pads): The electrical conductivity of carbon-based nanomaterials is intrinsic, ranging from $\sigma > 10^3 S/m$, which are good conductors. The GNP network reaches the electrical percolation threshold at a loading fraction of $\sim 15\ vol\%$, and in the bulk composite, the material becomes electrically conductive.

3. Mitigation Architectures: For the proper use of GNP pads in electronic packaging, thermal designers need to utilise hybrid isolation architectures. They can involve co-moulding ultra-thin layers of insulating polyimide films or ceramic coating on the faces of the pads, or they could also confine the GNP pads in the electrically isolated module lids and heat spreaders.

Engineering Trade-offs: Mechanical Compliance, Cost, and Durability

The challenge for the transition of GNP thermal materials from laboratory prototypes to electronic devices in industry is balancing all three constraints: mechanical, economic, and operational, with thermal requirements:

1. Mechanical Compliance and Compression Set: They should be soft and conformable (low shore hardness) to reduce mechanical stress on delicate silicon dies when clamping force is applied, and effective TIMs. Too high a filler loading embrittles the polymer host. GNP pads have a higher degree of matrix flexibility and mechanical compliance as they exhibit high thermal performance at relatively low volume loading ($15\ vol\%$) as compared to ceramic powder ($50 - 70\ vol\%$). But with the cyclic compression/temperature expansion of carbon nanostructures, a permanent deformation (compression set) or pump-out from the matrix can occur that may compromise the interface with contact over time.

2. Cost and Material Efficiency: The technology of pure carbon nanotubes (CNTs) and single-layer graphene is still too expensive for mass-market thermal pads. GNPs can be obtained by liquid-phase or thermal exfoliation of natural graphite, which is a cost-effective process, and provides a good cost-performance ratio. In addition, replacing heavy metallic or ceramic fillers with low-weight carbon fillers means that the overall material mass is reduced, thereby directly contributing to the reduction of supply chain raw material intensity and lighter device assemblies.

3. Long Term Reliability: Real-world power electronics have continuous thermal cycling between ambient and peak operating temperatures. The present study also verified the run-to-run consistency after 5 technical heating/cooling cycles, but long-term degradation mechanisms (e.g., thermo-oxidative degradation of the host polymer, filler agglomeration, or interfacial delamination) require high-humidity bias testing under standard environmental stress screening (ESS) protocols to generate the extended thermal shock ($1000\ +$ cycles).

LIMITATIONS

The empirical results show a statistically significant decrease in the peak operating temperature and thermal resistance of the tested GNP composite, but several experimental caveats need to be noted:

1. Technical Replicate Scope: The five thermal runs ($N = 5$)were technical replicates, not different physical samples taken from different production runs. As a result, the high statistical significance ($t(4) = 86.79$)clearly supports the excellent repeatability of the test bench and the short-term thermal stability of these commercial GNP formulations, which has been confirmed, but this cannot be extended to other commercial GNP formulations or manufacturing batches.
2. Constant Power Load vs. Dynamic Workloads: The test bench used for experimental testing had a constant 12.0 W electrical power load placed for 15 minutes, as well as a constant $10.0\ W/cm^2$ static heat flux for 15 minutes. This configuration is used to measure the steady-state thermal resistance under uniform heat flux conditions; however, to model the dynamic, real-world processor workloads characterised by frequent, non-linear changes in power and by repeated thermal expansion/contraction cycles is not simulated.

3. Single Environmental Condition: All tests were made in a climate-controlled laboratory enclosure at a fixed ambient temperature of $28.04^{\circ}C \pm 0.3^{\circ}C$. Extreme environmental conditions, sub-zero operation and high-humidity bias environment were not considered in the study.
4. Short-term thermal runs (15 minutes) are not a method for capturing long-term physical failure mechanisms inherent in elastomeric pads, including polymer matrix thermo-oxidative hardening, mechanical compression set under continuous clamping torque ($0.3\ N \cdot m$), silicone oil bleed, and interfacial delamination after 1000+ thermal shock cycles.
5. Electrical Safety Constraints: No experimental measurements of the electrical properties of the bulk GNP pad were performed. The intrinsic short circuit risk of the pad is present if the pad is attached to exposed IC traces without the addition of an integral dielectric isolation barrier because carbon-based fillers reduce electrical volume resistivity below the percolation threshold (~15 vol%).
6. Two-Point Temperature Sensing: Only two-point thermocouple probes T_{hot}, T_{cold} were used to measure the temperature, located at the contact interface. This method gives accurate global R_{th} results, but is unable to resolve local spatial temperature gradients or variations in heat spreading due to localised anisotropies within the pad surface.

CONCLUSION

This study conducted a direct, empirical performance evaluation comparing a graphite nanoplatelet (GNP)-reinforced composite thermal pad (~20 wt%, ~15 vol% filler loading in a silicone matrix) against a conventional ceramic-filled silicone control pad under continuous, fixed active heat flux ($12.0\ W$, $10.0\ W/cm^2$).

Key Findings

1. Peak Temperatures & Thermal Elevation: The introduction of GNP filler additives resulted in a significant lowering of the mean maxima interface operating temperature from $56.22 \pm 0.51\ ^{\circ}C$ (control ceramic) to $46.34 \pm 0.42\ ^{\circ}C$(GNP composites), which equates to a decrease in absolute interface operating temperature of 9.88 °C. Within controlled lab ambient conditions ($T_{ambient} = 28.04 \pm 0.3\ ^{\circ}C$), ΔT dropped from $28.18 \pm 0.51\ ^{\circ}C$ to $18.30 \pm 0.42\ ^{\circ}C$, which is a 35.06% decrease in thermal elevation.
2. Thermal Resistance & Impedance: Based on steady state heat transfer principles (ASTM D5470), the interface thermal resistance (R_{th}) was determined to be $1.53 \pm 0.04\ K/W$, and the area-normalised thermal impedance (Z_{th}) was $1.84\ K \cdot cm^2/W$ in the GNP composite. By contrast, the commercial ceramic control material had $R_{th} = 2.35 \pm 0.04\ K/W$ and

$Z_{th} = 2.82\ K \cdot cm^2/W$, which represents a 34.89% decrease in thermal resistance by the GNP material.

3. Transient Equilibrium and Thermal Stabilisation: Using an objective criterion of mathematical threshold value for equilibrium ($dT/dt < 0.1\ ^\circ C/min$), the graphene nanoplatelet (GNP) composite thermal pad reached steady state thermal equilibrium within 10 minutes (600 s), thus, achieving 33.3% higher stabilisation rate than the ceramic control thermal pad that needed around 15 minutes (900 s).
4. Statistical Hypothesis Testing: The results obtained allowed rejection of the Null Hypothesis (H_0), which postulated that there is no statistically significant difference in both thermal rise (ΔT) and interfacial thermal resistance (R_{th}) between thermal pads with GNP enhancement and ordinary silicone rubber pads under the same heat flux of $10.0\ W/cm^2$. In accordance with a two-tailed paired-samples t-test, the performance improvement is statistically significant to a high degree ($t(4) = 86.79,\ p = 1.34 \times 10^{-7},\ Cohen's\ d = 21.2;\ 95\%\ CI$: $[9.58\ ^\circ C,\ 10.18\ ^\circ C]$), proving that two-dimensional carbon nanoparticles significantly enhance heat transfer through the interface in the test bed configuration.

Practical Implications

While these results demonstrate that 2D carbon nanoplatelet fillers significantly enhance interface heat transport compared to standard spherical ceramic particles under continuous steady-state loads, the findings reflect sequential technical replicates ($N = 5$) conducted on a single product pair test bench setup. Consequently, statistical significance confirms exceptional test-bench repeatability and short-term thermal stability rather than broad population generalisation across disparate commercial batches.

For practical industrial deployment in high-density electronics packaging, thermal engineers must account for the intrinsic electrical conductivity of graphite fillers. Implementing hybrid isolation architectures (e.g., co-moulded dielectric polyimide barriers) will be essential to prevent short-circuit risks on active semiconductor die traces. Furthermore, future research must extend beyond constant-power laboratory screening to evaluate multi-specimen batches under dynamic power cycling and extended environmental stress conditions.

Recommendations

- Experimental evidence of the ability of graphite nanoplatelet (GNP) composites to lower steady state thermal resistance and peak operating temperatures under constant heat flux is promising, but thermal engineers and packaging designers should consider using the results as motivation to continue screening multiple specimens before using the technology for commercial products.
- **Dynamic Power Cycling Tests**: Future work needs to address GNP composite pads under dynamic transient power cycling (e.g. stepped or pulsed heat loads) rather than sustained constant

heat flux, which is reflective of actual workloads where electronic devices have continuous thermal fluctuations.

- **Extended Duration & Ageing Studies:** Further studies should be conducted for a longer test time to investigate long-term reliability degradation phenomena unique to solid elastomeric pads, including compression set under sustained clamping pressure, thermo-oxidative matrix hardening, silicone oil bleed, and thermal stress-induced delamination.
- **Environmental Stress Screening:** Dielectric isolation and contact testing should be expanded beyond controlled environmental laboratory ambient conditions (28.04˚C) to include standard industrial operating temperature ranges (0˚C to 85˚C) and environmental stress testing (such as high-humidity bias testing).

REFERENCES

ASTM International. (2017). *Standard test method for thermal transmission properties of thermally conductive electrical insulation materials* (ASTM D5470-17). ASTM International, West Conshohocken, PA. https://doi.org/10.1520/D5470-17

Chang, T. C., Fuh, Y. K., & Tu, S. X. (2017). Screen-printed graphite nanoplatelet and nanoparticle composites for thermal interface materials application. *Journal of Materials Science: Materials in Electronics*, 28(20), 15610–15617. https://doi.org/10.1007/s10854-017-7451-z

Lin, C. A., & Chung, D. D. L. (2009). Graphite nanoplatelet pastes vs. carbon black pastes as thermal interface materials. *Carbon*, 47(6), 1590–1595. https://doi.org/10.1016/j.carbon.2009.02.012

Prasher, R. (2006). Thermal interface materials: Historical perspective, status, and future directions. *Proceedings of the IEEE*, 94(8), 1571–1586. https://doi.org/10.1109/JPROC.2006.879796

Raza, M. A., Westwood, A. V. K., & Stirling, C. (2010). Graphite nanoplatelet/silicone composites for thermal interface applications. *2010 International Symposium on Advanced Packaging Materials: Microtech (APM)*, 34–48. https://doi.org/10.1109/ISAPM.2010.5441382

Raza, M. A., Westwood, A. V. K., & Stirling, C. (2018). Composites of graphite nanoplatelets and rubbery epoxy resins as adhesives and pads for thermal interface material applications. *Journal of Materials Science: Materials in Electronics*, 29(11), 8903–8912. https://doi.org/10.1007/s10854-018-8903-8

Shahil, K. M., & Balandin, A. A. (2012). Graphene–multilayer graphene nanocomposites as highly efficient thermal interface materials. *Nano Letters*, 12(2), 861–867. https://doi.org/10.1021/nl2039065

Tian, X., Itkis, M. E., & Haddon, R. C. (2015). Application of hybrid fillers for improving the through-plane heat transport in graphite nanoplatelet-based thermal interface layers. *Scientific Reports*, 5(1), Article 13108. https://doi.org/10.1038/srep13108